ISSN 1063-7834, Physics of the Solid State, 2012, Vol. 54, No. 7, pp. 1494–1500. © Pleiades Publishing, Ltd., 2012.
Original Russian Text © Yu.E. Greben'kova, A.V. Chernichenko, D.A. Velikanov, I.A. Turpanov, E.Kh. Mukhamedzhanov, Ya.V. Zubavichus, A.K. Cherkov, G.S. Patrin, 2012, published in Fizika Tverdogo Tela, 2012, Vol. 54, No. 7, pp. 1405–1411.

Ni–Ge Nanostructures: Role of the Interface and the Magnetic Properties

Yu. E. Greben'kova[a], *, A. V. Chernichenko[a], D. A. Velikanov[a, b], I. A. Turpanov[a], E. Kh. Mukhamedzhanov[c], Ya. V. Zubavichus[c], A. K. Cherkov[d], and G. S. Patrin[a, b]

[a] *Kirensky Institute of Physics, Siberian Branch of the Russian Academy of Sciences, Akademgorodok 50–38, Krasnoyarsk, 660036 Russia*

* *e-mail: uliag@iph.krasn.ru*

[b] *Siberian Federal University, pr. Svobodnyi 79, Krasnoyarsk, 660041 Russia*

[c] *National Research Centre "Kurchatov Institute," pl. Akademika Kurchatova 1, Moscow, 123182 Russia*

[d] *Boreskov Institute of Catalysis, Siberian Branch of the Russian Academy of Sciences, pr. Akademika Lavrentieva 5, Novosibirsk, 630090 Russia*

Received September 29, 2011; in final form, November 18, 2011

Abstract—The surface morphology and local structure of layers in the Ni–Ge and Ge–Ni–Ge–Ni–Ge films have been investigated. It has been shown that the surface of the films follows the roughnesses of the substrate surface, which have characteristic dimensions of 2–4 nm in height and ~100 nm in plane. It has been found that an interface with the depth ranging from 9 to 18 nm is formed at the boundaries between the Ni and Ge layers. The data obtained have been used to explain the specific features of the magnetic properties of the studied films, such as the asymmetry of hysteresis loops at low temperatures and the difference between the temperature dependences of the magnetization of the samples for two cooling modes: in a magnetic field and without a magnetic field.

DOI: 10.1134/S1063783412070177

1. INTRODUCTION

The processes occurring at the boundaries of the metal and semiconductor layers in hybrid structures have attracted considerable attention due to their influence on the properties of structures that have been widely used in microelectronic devices. In particular, nickel silicide layers have been used in integrated circuits as ohmic contacts or mutual elements in complementary metal–oxide semiconductor (CMOS) transistors [1]. A higher mobility of holes and electrons in germanium as compared to silicon can provide better properties of contacts based on nickel germanides [2]; therefore, many authors have intensively investigated interface layers in Ni–Ge structures (see, for example, [3–5]). In addition to specific electrical properties associated with interface layers, hybrid structures can exhibit new magnetic properties. In our previous investigations of magnetic and magneto-optical properties of two-layer and five-layer Ni–Ge films [6, 7], we revealed an abrupt increase in the coercive force and an asymmetry of the hysteresis loop at low temperatures, dependences of the magnetization and the Faraday effect on the thickness of an intermediate germanium layer in five-layer samples, and different temperature dependences of the magnetization of the films for two cooling modes: in a magnetic field and without a magnetic field. Presumably, these specific features are associated with the influence of a transition layer between the Ni and Ge layers. This paper is devoted to the investigation of the surface morphology and local structure of Ni–Ge films with the purpose of elucidating the mechanisms responsible for the observed specific features of the magnetic and magneto-optical properties.

2. SAMPLE PREPARATION AND EXPERIMENTAL TECHNIQUE

For our experiments, the films were prepared by ion-plasma sputtering of nickel and germanium from individual targets at a base pressure of 10^{-6} Torr in a vacuum chamber in an argon atmosphere. Cover glasses and special glasses purchased from Asahi company were used as substrates. The temperature of the substrates during the deposition was equal to 373 K. Tables 1 and 2 presents the thicknesses of the studied five-layer and two-layer Ni–Ge films, respectively. The surface morphology of the substrates and deposited films was examined using a Veeco MultiMode atomic force microscope. The local atomic structure of the Ni–Ge films was investigated using extended X-ray absorption fine structure/X-ray absorption near edge structure (EXAFS/XANES) spectroscopy and X-ray reflectometry with synchrotron radiation on the "Structural Materials Science" and "High-Precision X-Ray Optics" stations installed at the Kurchatov

Synchrotron Radiation Source, as well as using an JEM-4000 EX electron microscope at an accelerating voltage of 400 keV in the cross-sectional configuration. During the preparation for the electron microscopy examination, the sample was polished to a thickness of 30–50 μm, followed by thinning on a Gatan PIPS ion etching system until an opening was formed. After this treatment, the edges of the opening contained regions with a thickness of several tens of nanometers, which were transparent to electrons. The magnetization was measured on an MPMS XL magnetometer at temperatures in the range from 4.2 to 273 K in a magnetic field H up to 1 kOe. The measurements of the temperature dependences of the magnetization were carried out in two cooling modes: (1) the sample was cooled in a magnetic field (FC); and (2) the sample was cooled in zero magnetic field (ZFC). The magnetization measurements were performed during heating in the same magnetic field as was used in the FC mode.

3. RESULTS AND DISCUSSION

The atomic force microscopy investigation of the samples has revealed that surfaces of both types of substrates are characterized by a granular-type relief. The surface of the film follows the structure of the substrate surface. Figure 1 shows the top view of the surface of sample no. 7 and the distribution of heterogeneities along the line marked by triangles. It can be seen from this figure that heterogeneities with a height of 2–4 nm and in-plane dimensions ranging from 100 to 300 nm are predominant on the surface of the sample. The order of deposition of layers does not significantly affect the structure of the films.

The specific features of the local environment of nickel and germanium atoms in the films can be revealed by analyzing the EXAFS/XANES spectra. The EXAFS/XANES spectra were measured for a series of two-layer films (samples nos. 1, 3, and 4) at the K absorption edges of nickel and germanium. The germanium K-edge spectra of the two-layer films are closely similar to each other and are also similar to the spectrum of the reference sample, i.e., bulk germanium. At the same time, the spectra measured at the Ni K absorption edge of the films differ significantly from the spectrum of the nickel reference sample, and the degree of difference correlates with the thickness of the deposited nickel layer: the maximum differences are observed for two-layer film no. 1 (d_{Ni} = 8 nm). In the Ni K-edge XANES spectra (Fig. 2a), this manifests itself in the form of a substantial transformation of the fine structure without a significant shift of the absorption edge, which indicates a redistribution of the electron density at the nickel atoms, for example, due to the formation of the intermetallic compound Ni_xGe_y, without a significant change in the oxidation state.

Table 1. Thicknesses (in nm) of layers in five-layer Ni–Ge samples

Layer	Sample no.						
	1	2	3	4	5	6	7
Ge	17.6	20	20	46.1	20	20	47.7
Ni	9.7	16.3	15.5	26.5	16	18	15.5
Ge	1.7	2	3.5	6.3	7.6	10	26.0
Ni	9.7	16.3	15.5	26.5	16	18	15.5
Ge	17.6	20	20	46.1	20	20	47.7

Table 2. Thicknesses (in nm) of layers in two-layer Ni–Ge samples

Layer	Sample no.				
	1	2	3	4	5
Ge	46.5	46	46	48.5	13
Ni	8	15	17	26.5	20

The Fourier transforms of the EXAFS spectra (Fig. 2b) are characterized by the dependence of the height of the peak attributed to the first coordination sphere on the thickness of the film: the smaller is the thickness of the nickel layer, the lower is the height of the peak. In the spectra of films nos. 3 and 4 (curve *4* in Fig. 2b), there are clearly pronounced maxima in the range 3–5 Å, which correspond to the distant coordination spheres in the structure of face-centered (fcc) nickel. For sample no. 1 (curve *1* in Fig. 2b), the spectrum exhibits more diffuse maxima. By analyzing the these data in combination with the XANES data, the observed picture can be explained by the fact that a rather broad interface region of the intermetallic compound Ni_xGe_y is formed at the boundary between the nickel and germanium layers of the film, so that the relative contribution of this region increases with a decrease in the thickness of the nickel layer. Thus, the thickness of the nickel layer without germanium inclusions (hereinafter, it will be referred to as the effective

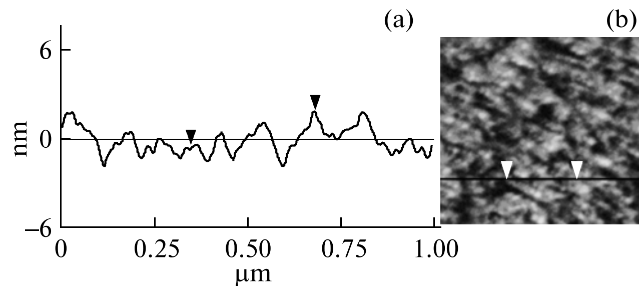

Fig. 1. (a) Size distribution of heterogeneities in the plane of sample no. 7 and (b) top view of the surface of sample no. 7.

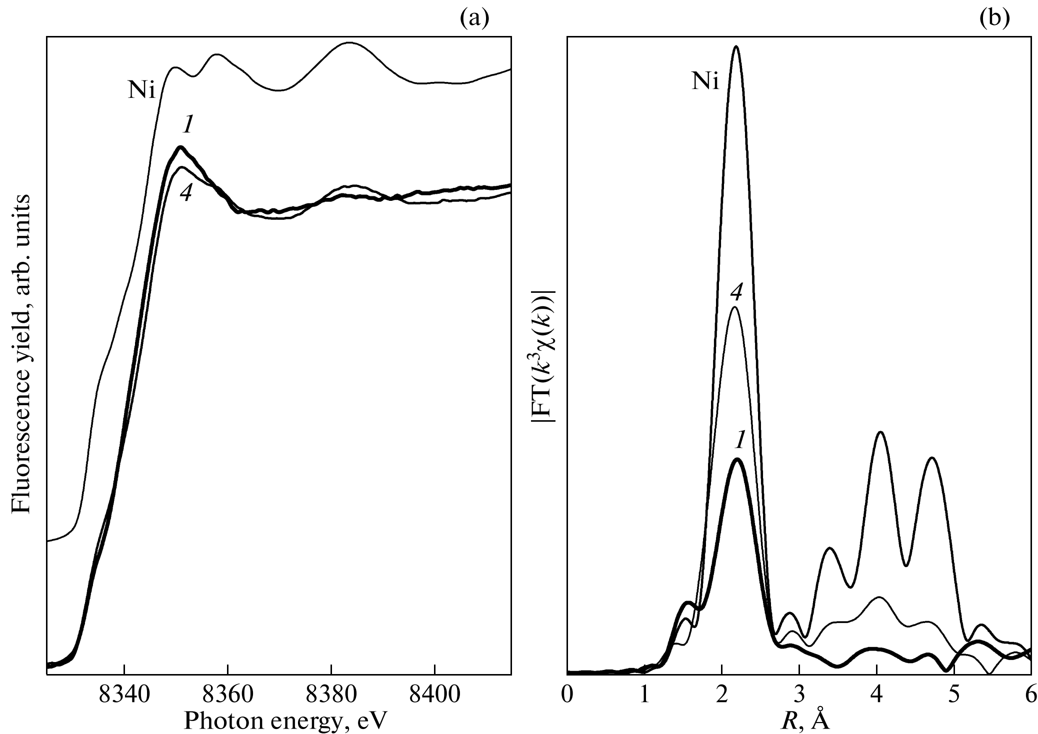

Fig. 2. (a) Ni *K*-edge XANES spectra and (b) Fourier transforms of the EXAFS spectra for two-layer Ni–Ge films nos. 1 and 4 in comparison with the nickel reference sample. Numbers of the curves correspond to the numbers of the samples.

thickness) decreases significantly as compared to the thickness specified for the deposition. For two-layer film no. 1, the vast majority of nickel atoms pass into the interface phase. For all the two-layer films under investigation, the thickness of the germanium layer is significantly larger than the thickness of the nickel layer; therefore, the effects of formation of the interface layer hardly manifest themselves in the XANES/EXAFS spectra measured at the *K* absorption edge of germanium. The absence of characteristic peaks to the left of the main peak in the spectra allows the conclusion that these film structures do not contain nickel oxide.

The angular dependences of the X-ray reflection intensity of two-layer samples nos. 1, 3, and 4 are shown in Fig. 3. These dependences exhibit the main tendency toward a decrease in the intensity of the reflected signal as a function of the angle of incidence with the interference peaks observed against the background of the overall pattern. The number of peaks depends on the total thickness of the system: in our case, the larger is the thickness of the nickel layer, the larger is the number of characteristic peaks (the thickness of the germanium layer remains almost unchanged for all the samples under investigation). The presence of several pronounced periods of oscillations in these dependences usually indicates that there are several clearly defined boundaries. At the same time, the sharpness of individual peaks (their dispersion) implies the sharpness of the heterointerfaces. Such a pattern can also indicate the formation of an intermediate layer (interface) between the nickel and germanium layers with relatively sharp well-reflecting boundaries. In turn, this suggests the formation of the Ni_xGe_y compound in the layer under consideration, rather than the gradual change in the concentration of nickel and germanium during the transition from layer to layer. A similar formation of a broad interface from a particular compound in the Ni–Ge structures was observed earlier in a number of works [4, 5].

Figure 4 shows the calculated angular dependences of the X-ray reflection intensity for two cases—a sharp boundary between the nickel and germanium layers (curve *1*) and a broad interface with rough boundaries (curve *2*)—in comparison with the experimental curve for two-layer sample no. 2 (curve *3*). Curves *1* and *2* were calculated according to the special program with the thicknesses of two layers (Ge and Ni) used as fitting parameters in the first case and the thicknesses of three layers (Ge, Ni_xGe_y, Ni) in the second case; in addition, the roughness of the surfaces was also taken into account. For the first case, we could not achieve satisfactory agreement between the calculated and experimental curves. For the second case, the calculated curve *2* coincides satisfactorily with the experimental curve *3* for the values of the fitting parameters presented in Table 3. It can be seen from this table that, in sample no. 2, the calculated depth of the Ni_xGe_y

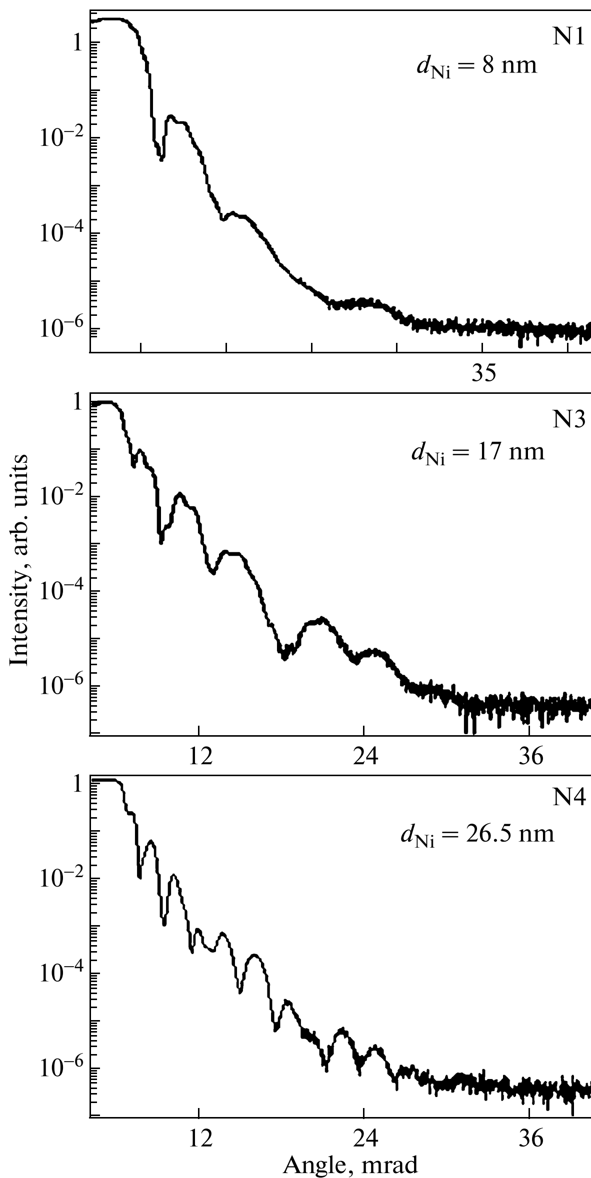

Fig. 3. Angular dependences of the X-ray reflection intensity of two-layer films nos. 1, 3, and 4.

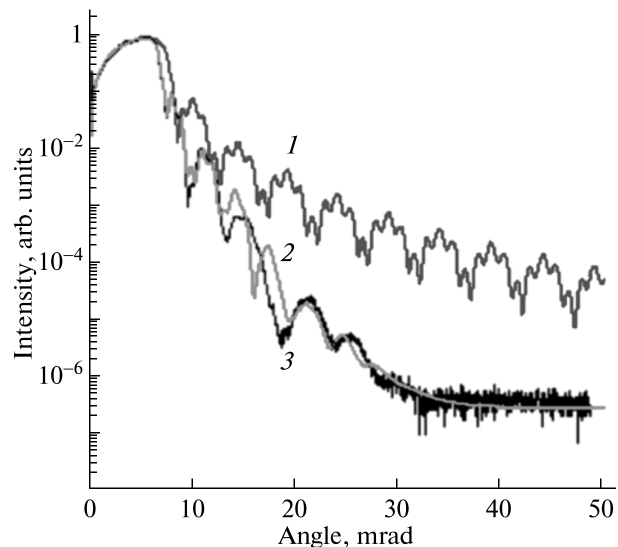

Fig. 4. Calculated and experimental angular dependences of the X-ray reflection intensity of two-layer film no. 2: (*1*) calculated curve for a two-layer structure with the atomic boundary between the Ni and Ge layers, (*2*) calculated curve for a structure containing the intermediate Ni_xGe_y layer, and (*3*) experimental curve of the angular dependence of the X-ray reflection intensity.

interface is equal to 9 nm. It should be noted that the depth of the interface in different samples can vary depending on the conditions used for their preparation. Nonetheless, for sufficient thicknesses of the nickel and germanium layers, the depth of the interface in all the studied samples should be close to the aforementioned value, because the controlled parameters of the film deposition were held to be constant.

Based on the data obtained in this study, we can construct the actual distribution of components in the Ni–Ge samples. Figure 5 shows the schematic representation of the distribution of components in the cross section of the five-layer film samples in which the thickness of the intermediate germanium layer is varied but the thicknesses of the other layers remain unchanged. In the case where the thickness of the intermediate germanium layer is sufficiently large, the Ni_xGe_y interfaces are formed at the layer boundaries (Fig. 5a). As the thickness of this layer decreases, the intermediate interfaces merge together (Fig. 5b). For both cases, the effective thickness of nickel layers is reduced as compared to the thickness corresponding to the deposition parameters. With a further decrease in the thickness of the intermediate germanium layer, the interface between the nickel layers becomes narrower, while the effective thickness of the nickel layers increases (Fig. 5c). This situation is completely consistent with the decrease in the Faraday effect with an increase in the thickness of the intermediate germanium layer, which was actually observed in our earlier work [8] (Table 4). By using this scheme, we can also explain twice the thickness (~18 nm) of the interface in five-layer film no. 4 observed using an electron microscope (Fig. 6), as compared to the thickness of the interface in the two-layer film (~9 nm). These cases are schematically illustrated in Figs. 5b and 5c, respectively. A significant excess of the thickness of the interface with respect to the thickness of the intermediate germanium layer (6.3 nm) indicates a higher nickel content in the Ni_xGe_y compound; i.e., the NiGe phase in this sample is not formed.

Thus, the structural data obtained for the samples under investigation allow us to draw the following conclusions: (1) an intermediate layer with a thickness of approximately 9 nm, which is uniform in composition and has sharp boundaries, is formed between the nickel and germanium layers; (2) in the case where the

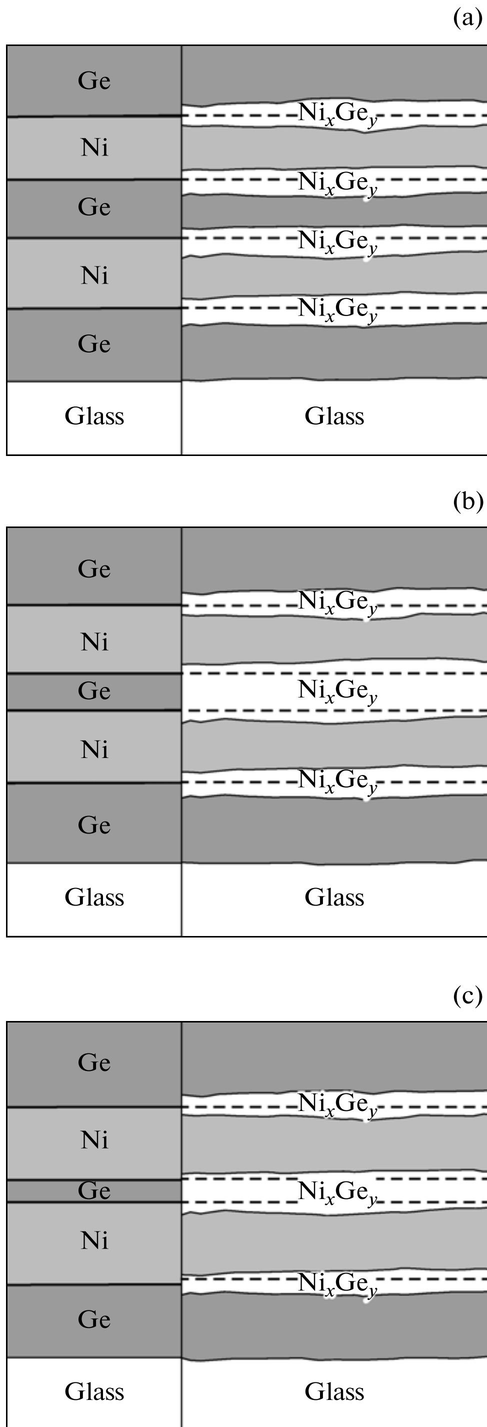

Fig. 5. Schematic representation of the distribution of components in the cross section of the five-layer film samples with different thicknesses of the intermediate germanium layer (the layer thickness decreases from panel (a) to panel (c); for details, see the text). The left column in each panel corresponds to nominal parameters of the arrangement of the layers, and the right column corresponds to the actual distribution of the components. The uneven boundaries between the layers are roughnesses observed using an atomic force microscope and evaluated from the reflectometry data (Table 3).

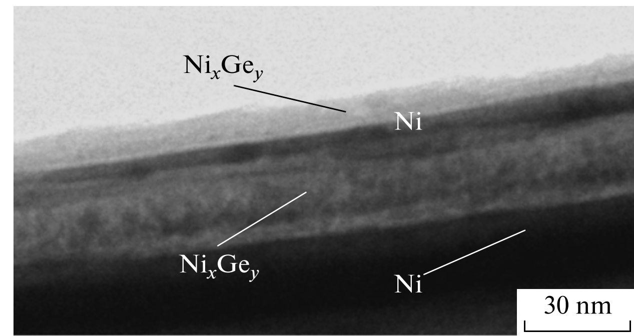

Fig. 6. Electron microscopy image of a fragment of the cross section of five-layer sample no. 4.

germanium layer is sandwiched between two nickel layers, the limiting thickness of the interface increases and can reach twice the thickness of the interface in the two-layer film; (3) the layer surfaces are rough; and (4) nickel oxide is not observed. These results can be used to explain the specific features of the field and temperature dependences of the magnetization of the studied films, such as the asymmetry of hysteresis loops at low temperatures and the difference between the temperature dependences of the magnetization measured in the low-temperature range in the FC and ZFC modes. Examples are shown in Figs. 7 and 8, respectively. The degree of asymmetry of the hysteresis loop depends on the thickness of the nickel layer: the smaller is the thickness of the nickel layer, the larger is the shift of the hysteresis loop along the axis of magnetic fields.

It can be seen from Fig. 8 that the FC curve (curve *1*) demonstrates a slow increase in the magnetization with a decrease in the temperature, which is characteristic of bulk nickel. The FC and ZFC curves coincide with each other at temperatures T exceeding a particular temperature T_m. The temperature T_m is approximately identical for the samples with different thicknesses of the intermediate germanium layer [8]; however, it depends on the strength of the magnetic field and its direction with respect to the film surface. When the magnetic field decreases, the temperature T_m increases.

The first of the aforementioned effects is usually observed in film structures consisting of either ferromagnetic (FM) and antiferromagnetic (AFM) layers or soft magnetic and hard magnetic ferromagnetic layers and can be explained by the exchange interaction between the layers, i.e., by the so-called exchange anisotropy [9, 10]. The appearance of this anisotropy in the case under consideration could be attributed to the formation of an antiferromagnetic NiO layer [11]. However, as was shown above, these samples do not contain nickel oxide. The interaction between the nickel layers through the system of conduction of the germanium layer should also be rejected, because the

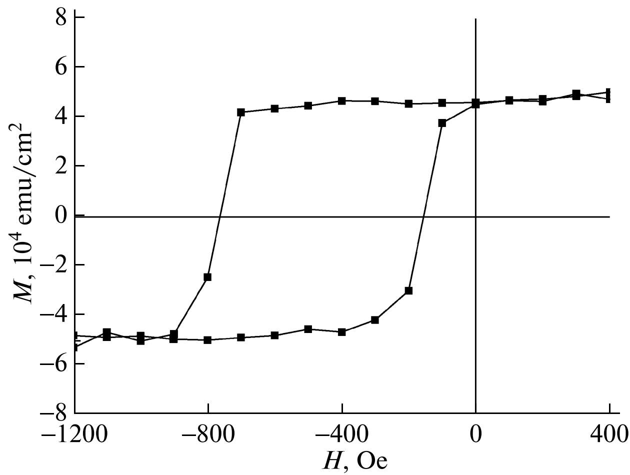

Fig. 7. Hysteresis loop of two-layer sample no. 5 at temperature $T = 5$ K. The magnetic field is applied parallel to the sample plane.

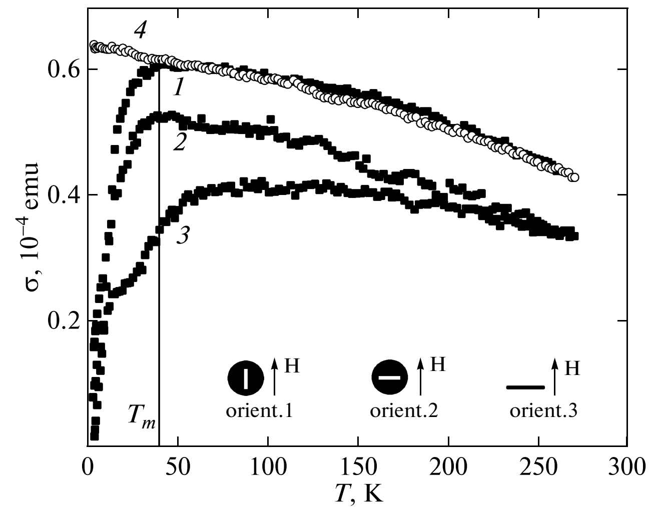

Fig. 8. Temperature dependences of the magnetization measured for sample no. 1 in the cooling modes (*1*–*3*) ZFC and (*4*) FC. The applied magnetic field during the measurement of the magnetization (ZFC mode) is oriented (*1*) parallel to the film plane along the easy magnetization axis, (*2*) parallel to the film plane along the hard magnetization axis, and (*3*) normal to the film plane. $H = 600$ Oe.

exchange shift of the hysteresis loops takes place in both the two-layer and five-layer films. The observed specific features could be assigned to the formation of an antiferromagnetic order in the interface with a decrease in the temperature. Thus, it is reasonable to assume that the Ni_xGe_y compound with the Néel temperature $T_N = 40$–60 K is formed in the interface, as is the case with the Fe–Ge and Mn–Ge compounds [12–14].

This assumption explains the asymmetry of the hysteresis loop, but it is not sufficient for the explanation of the difference between the temperature dependences of the magnetization measured in the FC and ZFC modes. Let us invoke the mechanism that was proposed in [15] and is related to the roughness of the boundary between the ferromagnetic and antiferromagnetic layers. In [15], the authors considered the situation with a stepped boundary between the ferromagnetic and antiferromagnetic layers in the film and showed that, in the ferromagnetic layer, there can arise a new type of domains with different magnetization orientations when the spins of the ferromagnetic layer in all regions of the boundary are aligned with the spins of the antiferromagnetic layer. In our case, the film surface is characterized by roughnesses with a height of 2–4 nm. These roughnesses also exist at the boundaries of the interface (Table 3). At temperatures $T > T_N$, the Ni_xGe_y layer is paramagnetic; the directions of magnetic moments of atoms in this layer are randomly distributed and do not affect the magnetization of the ferromagnetic layer, which increases with a decrease in the temperature, as is the case with bulk metallic nickel. At temperatures $T < T_N$, the Ni_xGe_y layer has an antiferromagnetic order. Because of the roughness of the boundary between the Ni and Ni_xGe_y layers, atoms of the antiferromagnetic layer in different regions of the boundary are located in different sublattices, and the nearest neighbors of the atoms of the ferromagnetic layer can be atoms of the antiferromagnetic layer with the oppositely directed magnetic moments, as is schematically shown in Fig. 9. Consequently, the nickel layer (or a part of the nickel layer) is divided into regions with opposite directions of the

Table 3. Calculated parameters that satisfy the measured angular dependence of the X-ray reflection intensity for the two-layer film (sample no. 2) (Fig. 4)

Layer	Initial thickness, nm	Calculated thickness, nm	Calculated surface roughness, nm
Ni	15	12	1.4
Ni_xGe_y	0	9	–
Ge	46	42	0.75
Substrate	–	–	1.75

Table 4. Dependence of the Faraday effect on the thickness of the intermediate germanium layer in five-layer samples nos. 2, 3, 5, and 6

d_{Ge}, nm	FE
2	7.5
3.5	5.5
7.6	4.7
10	3.2

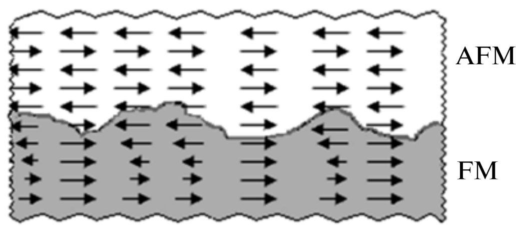

Fig. 9. Schematic representation of the situation that can occur at the rough boundary between the FM and AFM layers. The spins in the FM layer are aligned in accordance with the spins in the AFM layer at each point of the boundary.

magnetization and, during the cooling in zero magnetic field, the sample loses the total magnetic moment. During the heating in a magnetic field, the magnetic moments of atoms in the nickel layer are aligned along the field. The stronger is the magnetic field, the lower is the temperature at which the ordering occurs and the ZFC curve merges with the FC curve. A similar mechanism, which is associated with the FM–AFM coarse-grained surface of the boundary, was used in [16] for the explanation of the domain structure observed experimentally in the Mn film deposited on a stepped surface of the Fe(001) single crystal.

The proposed mechanism completely explains all the observed specific features of the magnetic properties of the studied films. However, in this work, we could not determine the exact composition and structure of the interface and to elucidate its magnetic properties. In the literature, reliable data on the magnetic properties of the Ni_xGe_y compounds are almost not available. A ferromagnetic order at room temperature with a small value of the magnetic moment was found in the bulk Ni_5Ge_3 sample prepared by mechanical milling and pressing [9]. The ferromagnetism and its variations under pressure in the Ni_3Ge compound were investigated in [17]. However, there exist many phases of nickel compounds with germanium [5], for which, in the literature, we have failed to find data on the type of magnetic ordering.

4. CONCLUSIONS

Thus, it has been shown that a broad interface Ni_xGe_y, which is approximately uniform in depth, is formed between the Ni and Ge layers of the films. The layers in the films are separated by rough interfaces. The specific features of the magnetic behavior of multilayer structures at low temperatures, such as the difference between the temperature dependences of the magnetization measured in the FC and ZFC modes and the asymmetry of hysteresis loops, have been explained by the formation of an interface with rough boundaries under the assumption that an antiferromagnetic order is formed at the interface in the temperature range from 40 to 60 K.

ACKNOWLEDGMENTS

This study was supported by the Russian Foundation for Basic Research (project nos. 11-02-00675 and 11-02-00972). The synchrotron investigations were performed on equipment of the Center for Collective Use "Kurchatov Center for Synchrotron Radiation and Nanotechnology" (state contract no. 16.552.11.7003).

REFERENCES

1. F. M. d'Heurle, C. S. Petersson, J. E. E. Baglin, S. J. La Placa, and C. Y. Wong, J. Appl. Phys. **55**, 4208 (1982).
2. S. Zhang, Microelectron. Eng. **70** (2), 174 (2003).
3. C. Perrin, D. Mangelincka, F. Nemouchia, J. Labar, C. Lavoie, C. Bergmana, and P. Gasa, Mater. Sci. Eng. B **154–155**, 163 (2008).
4. F. Nemouchi, D. Mangelinck, C. Bergman, G. Clugnet, and P. Gas, Appl. Phys. Lett. **89**, 131920 (2006).
5. S. Gaudet, C. Detavernier, C. Lavoie, and P. Desjardins, J. Appl. Phys. **100**, 034306 (2006).
6. I. S. Edel'man, G. S. Patrin, D. A. Velikanov, A. V. Chernichenko, I. A. Turpanov, and G. V. Bondarenko, JETP Lett. **87** (5), 262 (2008).
7. A. V. Chernichenko, D. A. Marushchenko, I. A. Turpanov, Yu. E. Greben'kova, and P. N. Mel'nikov, Zh. Sib. Fed. Univ., Ser. Mat. Fiz. **2**, 376 (2009).
8. I. S. Edelman, D. A. Velikanov, A. V. Chernichenko, D. A. Marushchenko, E. V. Eremin, I. A. Turpanov, G. V. Bondarenko, Yu. E. Greben'kova, and G. S. Patrin, Physica E (Amsterdam) **42**, 2301 (2010).
9. W. H. Meiklejohn and C. P. Bean, Phys. Rev. **105**, 904 (1957).
10. J. Nogues, J. Sort, V. Langlais, V. Skumryev, S. Surinach, J. S. Munoz, and M. D. Baro, Phys. Rep. **422**, 65 (2005).
11. L. Del. Bianco, F. Boscherini, M. Tamisari, F. Spizzo, M. V. Antisari, and E. Piscopiello, J. Phys. D: Appl. Phys. **41**, 134008 (2008).
12. K. Kanematsu and T. Ohoyama, J. Phys. Soc. Jpn. **20**, 236 (1965).
13. V. I. Nikolaev, S. S. Yakimov, I. A. Dubovtsev, and Z. V. Gavrilova, JETP Lett. **2** (8), 235 (1965).
14. A. Hjelm, J. Mod. Phys. B **7**, 1023 (1993).
15. A. I. Morosov and A. S. Sigov, Phys. Solid State **46** (3), 395 (2004).
16. U. Schlickum, N. Janke-Gilman, W. Wulfhekel, and J. Kirschneret, Phys. Rev. Lett. **92**, 107203 (2004).
17. T. Izumiy, M. Taniguchi, S. Kumai, and A. Sato, Philos. Mag. **84**, 3883 (2004).

Translated by O. Borovik-Romanova